Synthesis of graphene-like carbon from agricultural side stream with magnesiothermic reduction coupled with atmospheric pressure induction annealing

NANO EXPRESS

PAPER

Synthesis of graphene-like carbon from agricultural side stream with magnesiothermic reduction coupled with atmospheric pressure induction annealing

Anna Lähde[1], **Ondrej Haluska**[2], **Sara-Maaria Alatalo**[1], **Olli Sippula**[1], **Arūnas Meščeriakovas**[1], **Reijo Lappalainen**[2], **Tuomo Nissinen**[2], **Joakim Riikonen**[2] **and Vesa-Pekka Lehto**[2]

[1] University of Eastern Finland, Department of Environmental and Biological Sciences, 70210 Kuopio, Finland
[2] University of Eastern Finland, Department of Applied Physics, 70210 Kuopio, Finland

E-mail: anna.lahde@uef.fi

OPEN ACCESS

RECEIVED
7 February 2020

REVISED
18 March 2020

ACCEPTED FOR PUBLICATION
24 March 2020

PUBLISHED
7 April 2020

Keywords: agricultural side stream, biomass, graphitization, induction annealing, atmospheric pressure, magnesiothermic reduction, pyrolysis

Abstract

Generally, large-scale production of graphene is currently not commercially viable due to expensive raw materials, complexity and the high-energy consumption of the processes currently used in the production. The use of biomass precursors and energy efficient procedures for carbonization have been proposed to reduce the cost of the graphene materials. However, low-cost graphene production has not been accomplished yet. Herein, we present a sustainable procedure and renewable starting materials to synthesize carbon nanostructures with graphene-like features. First, a SiC/C composite was synthesized from phytoliths and sucrose through magnesiothermic reduction. The phytoliths were obtained from barley husk that is an abundant side stream of agricultural industry. Second, graphene-like structures were achieved by the graphitization of SiC/C composite with high temperature induction annealing at 2400 °C under atmospheric pressure. The formation of graphene-like carbon was initiated by vaporization of silicon from the pre-ceramic SiC/C. Complete transformation of SiC/C to hollow, spherical graphene-like carbon structures and sheets were verified with thermogravimetry, x-ray diffraction, energy dispersive spectroscopy, electron microscopy and Raman spectroscopy. Also, the theoretical thermodynamic consideration of the phase separation of silicon carbide and the role of free carbon in the process has been discussed.

1. Introduction

Graphene is a single atom layer thick sheet of carbon that was first found in 2004 [1, 2]. The unique electrical, thermal and optical properties of graphene combined with its mechanical integrity have attracted attention since its discovery [3]. Variable techniques have been reported to produce graphene but the most common techniques to produce graphene sheets, platelets and flakes still rely on methods such as exfoliation of graphite, epitaxial growth on SiC substrate and chemical vapor deposition (CVD). High-quality graphene is produced mainly with the energy intensive CVD method [4].

From the industrial production point of view these techniques suffer from high cost, low purity, heterogeneous features and limited upscaling [5, 6]. For this reason more sustainable and cost-efficient methods and starting materials are needed for the production of high purity graphene [7]. Utilization of biomass would reduce starting material cost but production of graphene from it is challenging particularly, when thermal treatment techniques are used. Thermally treated biomass typically results in partially ordered amorphous carbon/graphene stack composites, and carbon structures composing of randomly organized small crystalline domains. In addition, biomasses contain inherently heteroatoms (H/N/O/S) bound to carbon and other elements (K, Na, Mg, Fe etc), which can be problematic in the synthesis [8–10]. Therefore, approaches such as the use of catalysts or the pre-treatment of the biomass are required to obtain ordered graphitic or graphene-like

structures [11, 12]. Elements such as Mg, Fe, Ni or Si have been reported to direct carbonization towards graphitic structures [11, 13]. Especially silicon in the form of silicon carbide has been reported to favor the formation of graphene type carbon structures [2]. This reaction is usually conducted at high temperatures in vacuum. It is based on the sublimation of Si, leaving behind ordered carbon layers [4, 14, 15]. Pre-ceramic, nanocrystalline SiC is a promising starting material in the production of graphitic carbon structures as it favors the formation of high carbon content materials [16].

Nanostructured silicon carbide (nSiC) can be produced through several synthetic routes such as CVD, sol-gel process, thermal or laser ablation from organic compounds but also derived from biomass [17, 18]. However, current techniques often require expensive precursors, and toxic reactants that result in highly agglomerated nSiC particles [17, 19]. Magnesiothermic reduction (MTR) is an alternative method to produce nSiC according to the following pathway: $SiO_2(s) + C\ (s) + 2Mg\ (g) \rightarrow SiC(s) + 2MgO(s)$ [17]. It enables the production of nanostructured SiC with high purity, uniform size and morphology, while, strong agglomeration of the SiC particles can be prevented [17, 19–21]. Furthermore, MTR can be considered a sustainable approach to synthesize nSiC due to its low energy consumption, short reaction time and low temperature compared to the carbothermal reduction process known as the Acheson process [18, 22].

Herein, we report an alternative method for production of graphene-like carbon nanostructures from barley husk using magnesiothermic reduction coupled with atmospheric pressure induction annealing. First, the biomass based nanostructured silica ($nSiO_2$, phytoliths) was extracted from barley husk. Phytoliths are amorphous silica materials with porous structure that are produced by specific plants like barley, rice and sugarcane. Second, $nSiO_2$ and a small amount of carbohydrate in the form of sucrose was converted into silicon carbide/carbon composite (nSiC/C) using magnesiothermic reduction. Third, graphene-like structures were formed via nSiC/C dissociation at 2400 °C under atmospheric pressure using induction annealing. As the result, the formation of carbon materials through the complete removal of Si was accomplished and the product was a mixture of partially folded graphene-like and multi-layered carbon structures. For comparison, only partial removal of Si was observed with a crystalline, commercial SiC treated in similar conditions.

2. Materials and methods

2.1. Materials

Barley husk was obtained from Altia Oyj (Koskenkorva, Finland) as a side stream of their process. The chemicals used in the study were: 37% HCl (Merck), NaOH pellets (purity 99.5% Fisher Scientific), D(+)-Sucrose (AnalaR Normapur VWR Chemical), 95%–97% H_2SO_4 (J.T. Baker) and Mg powder $<$0.1 mm particles size (purity $\geqslant$ 97.0% Merck). Silicon carbide (SiC, 200–450 mesh particle size, Sigma Aldrich) was used as a crystalline SiC reference in the studies.

2.2. Extraction of silicon from barley husk

Nanostructured silica ($nSiO_2$) was produced from barley husk (BH). The BH was leached with 10% HCl at 100 °C for 2 h to remove inorganic impurities and hemicellulose. The HCl was removed by vacuum filtration and the solid material, $nSiO_2$, was washed with deionized water to remove chlorides after leaching. The washed $nSiO_2$ was dried at 100 °C and calcined in air at 550 °C.

2.3. Synthesis of nanostructured silicon carbide with high carbon content

Nanostructured silicon carbide/carbon composite (nSiC/C) was synthesized from the purified $nSiO_2$ and sucrose. First 28.6 g of sucrose was dissolved in 20.2 ml of 2.7 v-% H_2SO_4. Then $nSiO_2$ was added to this reaction solution in a mass ratio 1.2 sucrose/$nSiO_2$. This mixture was heated up to 160 °C for 5 h to enhance dehydration of sucrose to elemental carbon $C_nH_{2n}O_n + H_2SO_4 \rightarrow nC + H_2SO_4 + nH_2O$. To remove residual H_2O and decompose H_2SO_4, further treatment under N_2 atmosphere at 700 °C for 2 h was performed. Finally, magnesiothermic reduction was conducted in a custom-made reactor under N_2 atmosphere to obtain nSiC/C composite. Magnesium powder was mixed with the $nSiO_2$/C composite in mass ratio 2:1 and placed into the reactor. The temperature was increased to 100 °C and kept at this temperature for 30 min prior to the reduction. Reduction was initiated with a resistively-heated tungsten wire. The reaction propagated as high temperature reaction through the sample, in which maximum temperature within the powder reached 1000 °C. Synthesized nSiC/C was washed with 37% HCl at 70 °C for 1 h and 1 M NaOH at room temperature for 16 h to remove by-products, and dried at 65 °C for 2h.

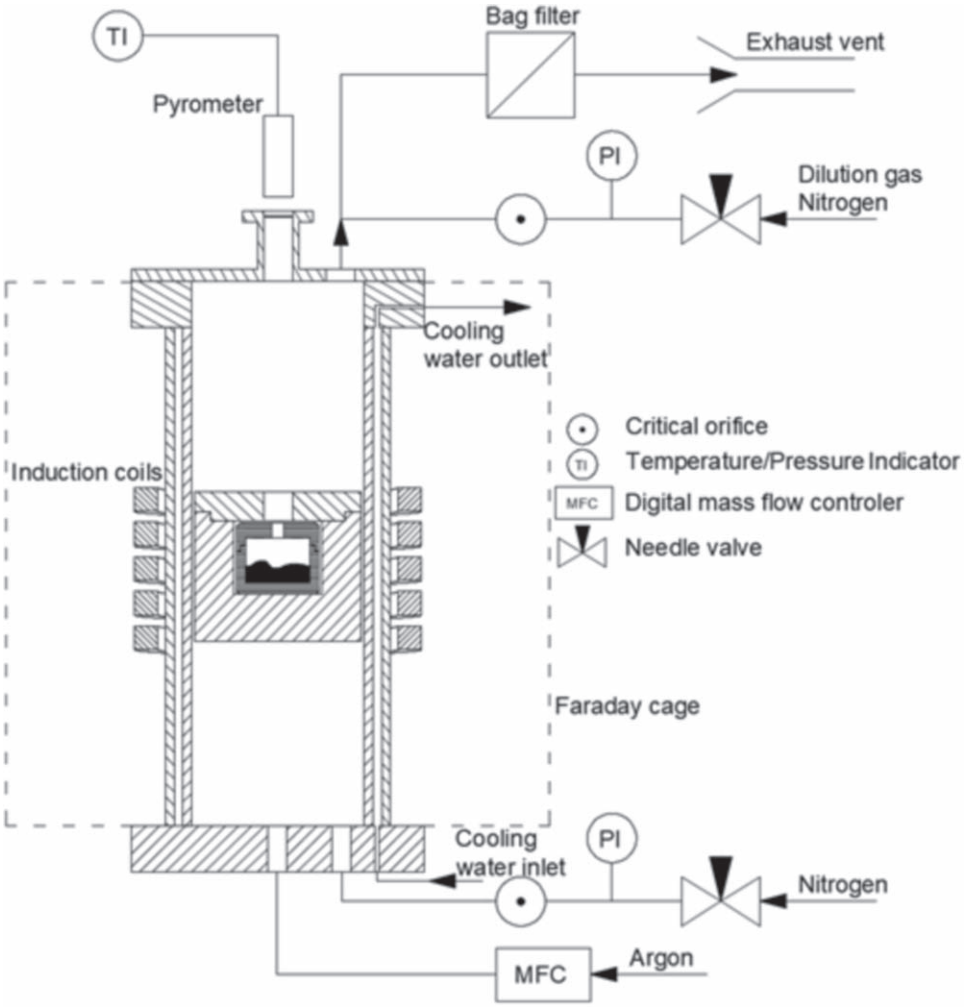

Figure 1. Schematic illustration of the experimental set up of the induction furnace. Sample is placed in graphite crucible, which is placed inside of the graphite felt thermal insulation. Induction annealing was performed under Argon atmosphere and atmospheric pressure. Sample was heated up to 2400 °C.

2.4. Graphitization of nanostructured silicon carbide/carbon composite by atmospheric pressure induction annealing

Conversion to graphene-like nanostructured carbon was achieved through induction annealing of the nSiC/C composite under atmospheric pressure in argon atmosphere. The induction furnace had 50 kW heating power. The induction annealing is an efficient high temperature treatment due to the high heat transfer capacity of induction [23]. The temperature of the sample was monitored with a Kleiber 730-LO pyrometer at temperatures between 350 °C and 2600 °C. The previously prepared nSiC/C powder (m = 0.5 g) was placed inside a graphite crucible, which was enclosed except for a small pyrometer view hole. The crucible was placed inside the induction oven between heating coils that generate an alternating magnetic field and heats up the crucible. The sample was heated up to 2400 °C under atmospheric pressure in Ar atmosphere and kept at this temperature for 20 min. Schematic illustration of the induction furnace is presented in the figure 1. More detailed explanation of induction annealing set up has been described elsewhere [16].

2.5. Characterization

Thermogravimetry analysis was performed with TA instruments TGA Q50. The measurements were performed under air, first at 80 °C for 30 min and followed by a heating ramp at 20 °C min^{-1} from 80 °C to 900 °C. The N_2 adsorption/desorption measurements were performed with Micromeritics Tristar II 3020 at 77 K. Before the N_2 sorption measurements the samples were degassed at 120 °C under vacuum for 1 h. The specific surface area was determined using the multipoint BET (Brunauer–Emmett–Teller) method.

X-ray powder diffraction examination was carried out with the Bragg-Brentano geometry utilizing the Bruker D8 Discover diffractometer equipped with Cu-tube, $\lambda = 1.54$ Å. Generator was set to 40 kV and 40 mA

and the K_β-radiation was removed with a 0.02 mm Ni-filter. The measurement was performed in the 2θ range 20°–90° with the step size of 0.038° and the step time of 1.2 s.

The structure of the particles was analyzed with scanning electron microscopy (SEM, Zeiss Sigma HDVP) and transmission electron microscopy (TEM, JEM-2100F JEOL Ltd). SEM imaging was conducted using 5 kV EHT, Inlens detector and WD 5 mm. Powder samples for SEM were placed on the aluminium stub and analyzed without coating. The size of the particles was estimated by measuring single particle sizes with ImageJ software. HSBD detector was used in the EDS studies. The TEM samples were prepared by pipetting a droplet of ethanol suspension to a holey carbon TEM grid. 200 kV acceleration voltage was used for the imaging.

Raman spectroscopy (Thermo DXR2xi Raman) was conducted at wavelength $\lambda = 532$ nm, 100× objective and 50 μm confocal pinhole aperture. Laser power of 2.5 mV and exposure time of 0.02 s were used in the analysis.

Thermodynamic equilibrium calculations were carried out with the Equilib-module of the FactSage 6.2 software in order to estimate the decomposition temperature of SiC, and its further reactions during the induction heating experiments. Thermodynamic data of the condensed and gas-phase species were taken from the Fact53 and Ftmisc-LMLQ (liquid light metal alloy) databases. The calculation was carried out at pressure of 1 bar and temperature range of 300 °C–3000 °C. During induction annealing the substance (SiC) is surrounded by argon gas. Therefore, the global equilibrium was calculated at SiC mixing ratio of 0.1 in argon gas. In addition, a local equilibrium without the presence of Argon gas was calculated.

3. Results and discussion

3.1. Production and properties of nanostructured silicon carbide/carbon composite

Synthesis of nSiC/C was carried out in two phases: (1) Extraction of nanostructured SiO_2 ($nSiO_2$) from agricultural side stream barley husk and (2) Production of nSiC/C composite through magnesiothermic reduction from $nSiO_2$ and sucrose. Barley husk is naturally rich in SiO_2 accumulated in phytoliths, which makes it an attractive source of SiO_2 [24]. However, prior to calcination barley husk must be acid-treated to remove metallic impurities, mainly Na and K to ensure high purity of the final product. These metallic impurities can form ternary oxides with SiO_2, e.g. $Na_6Si_8O_{19}$ or $Na_2Si_2O_5$ and consequently decrease the melting point of the ash during the heat treatment of the biomass. Presence of ternary oxides enable carbon in the biomass to dissolve and remain in such ternary oxides decreasing the purity of the final $nSiO_2$ product [25]. The extracted $nSiO_2$ was mixed with sucrose and treated under magnesiothermic reduction resulting in the formation of a nSiC/C composite. The mixture contained sucrose above the stochiometric amount needed for the formation of SiC in order to increase the amount of free carbon in the composite. This additional carbon improved the formation of graphitic structures in the induction annealing during the graphitization.

Figure 2 shows the thermogravimetric analysis, nitrogen adsorption-desorption isotherm and XRD diffractogram of the nSiC/C composite. Based on the analysis the total amount of free carbon in nSiC/C composite before induction annealing was 21 wt% (figure 2(A)). The nitrogen adsorption-desorption isotherm of nSiC/C resembled the type II isotherm with the H3 type hysteresis loop, which indicates mesoporous structures with BET surface area of $234 \pm 2\ m^2\ g^{-1}$ (figure 2(B)).

XRD analysis showed that nSiC/C composed of two different polytypes, namely SiC-3C and SiC-2H (figure 2(C)) [26–28]. The average crystallite size calculated from 2θ peaks 60.0° and 71.8° was 16.7 nm. In addition, a single diffraction peak of graphitic carbon was observed at 25.9°. The absence of the other diffraction peaks of graphitic carbon was due to the low crystallinity of the carbon in nSiC/C as can be expected based on the reaction temperature used in the magnesiothermic reduction (1000 °C).

Figure 3A and 3 show the SEM images of the nSiC/C composite. The nSiC/C appeared to be composed of sharp-edged crystals with the size varying between 100 nm and 600 nm, and spherically shaped primary particles forming larger porous structures. The elemental mapping conducted with energy dispersive x-ray spectroscopy (EDS) coupled with SEM indicated that the sharp-edged crystals composed of SiC and the porous structures were amorphous free carbon (figure 4(A)). The Mg peak in the EDS spectrum is due to a Mg residue from the magnesiothermic reduction and the Al peak is due to the SEM specimen stub. The oxygen peak may indicate the presence of unreacted SiO_2, MgO or silicon oxycarbide [29]. Also, some oxygen may be contributed by oxygen surface functional groups on free carbon.

3.2. Properties of graphitized carbon nanostructures formed by induction annealing at atmospheric pressure

Conversion of nSiC/C to graphene-like carbon was obtained with induction annealing at 2400 °C under Ar atmosphere and atmospheric pressure. XRD analysis showed formation of the highly graphitized carbon structures presented in figure 2(C). The diffraction peak at 83.5° particularly indicates the presence of the

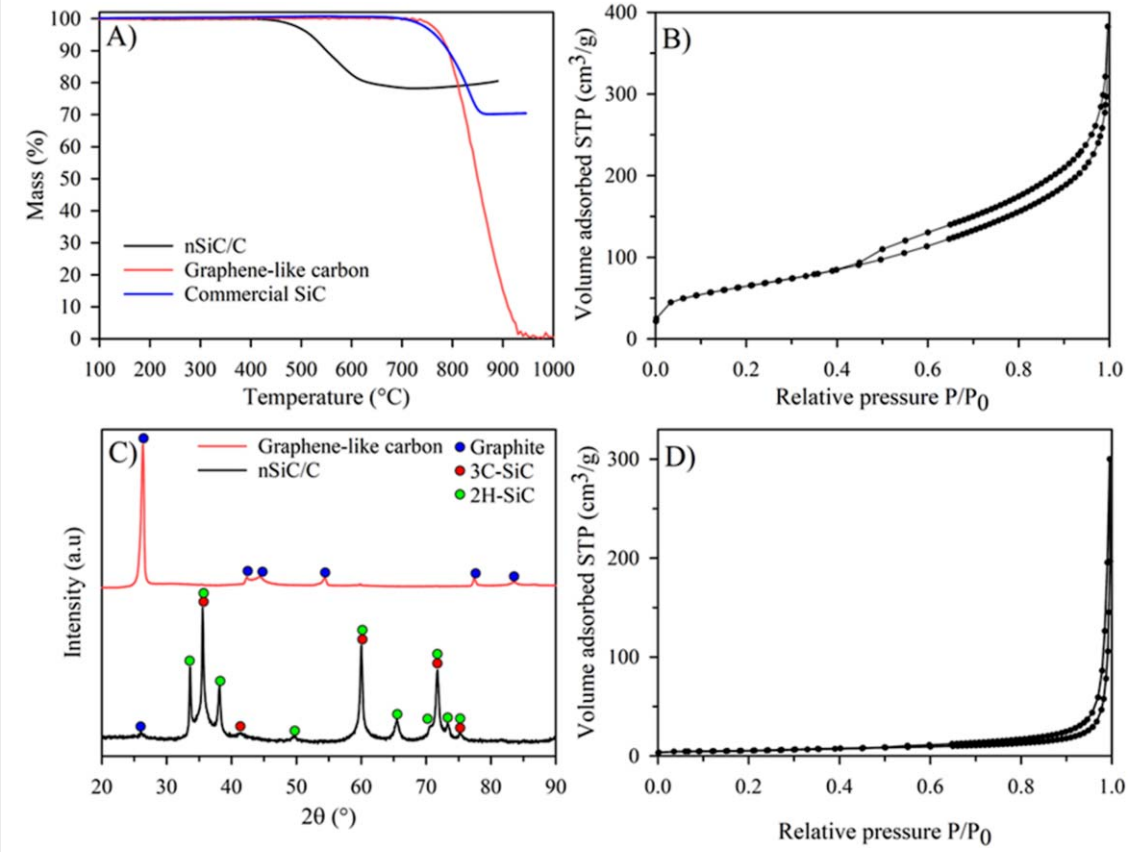

Figure 2. (A) TGA curve of nSiC/C before annealing, graphene-like carbon and commercial SiC after induction annealing, (B) Nitrogen adsorption-desorption isotherm of nSiC/C and, (C) XRD diffractograms of nSiC/C composite and graphene-like carbon and (D) Nitrogen adsorption-desorption isotherm of graphene-like carbon produced by induction annealing of nSiC/C.

multilayered carbon sheets as also seen in the TEM images (figures 3(C), (D)) [28]. As expected, the specific surface area of nSiC/C was reduced during the induction annealing as S_{BET} surface area of graphene-like carbon was only 19.0 $\pm$ 3 $m^2\ g^{-1}$. According to the nitrogen sorption-desorption isotherm (figure 2(D)) resembles the type III sorption isotherm referring to the non-porous or macroporous material.

The nSiC/C went through a complete morphological change as can be observed from the SEM images (figures 3(A) - (E)). The nSiC/C transformed mainly to hollow spherically shaped carbon structures with particle sizes varying from 50 to 500 nm in size. In addition to the spherical structures, sheet structures were observed as well as presented in figure 3(C). The atomic plane distance, based on the estimation from TEM images, between the multilayered carbon structures was 0.32 nm. This value is slightly lower than the atomic plane distance of crystalline graphite, which is 0.3354 nm [30].

Based on the Raman analysis shown in figure 3(F), there may be graphene domains present in the sample matrix in addition to the graphitic structures. Peak set up in Raman spectra correlated well with the values for graphene, i.e. dominant single Lorentzian 2D peak band at 2700.1 cm^{-1} with 24.4 cm^{-1} full width half maximum (FWHM) and G band at 1581.3 cm^{-1}. Minor D peak at 1349.8 cm^{-1} indicates minor defects in the material structure [31].

According to the thermogravimetric analysis complete conversion of nSiC/C composite to high carbon content material was achieved (figure 2(A)), which corresponds well to the results obtained from XRD and SEM-EDS analysis (figures 2(C) and 4(B)). This is significant improvement compared to the commercial SiC (Sigma-Aldrich) which resulted in only 25 wt% carbon conversion under similar thermal conditions (figure 2(A)). High conversion of nSiC/C to carbon achieved in this study is in a good agreement with our previous studies conducted with pre-ceramic, nanocrystalline SiC/C produced from organometallic compounds using the same induction annealing approach [16, 32].

3.3. Phase separation of silicon carbide and the role of free carbon

Figure 5 shows the thermodynamic equilibrium of bulk SiC under Ar atmosphere between 1600 °C and 3000 °C, based on the thermodynamic data of the condensed and gas-phase species provided in the Fact53 and Ftmisc-LMLQ (liquid light metal alloy) databases. According to the thermodynamic data, the decomposition of SiC

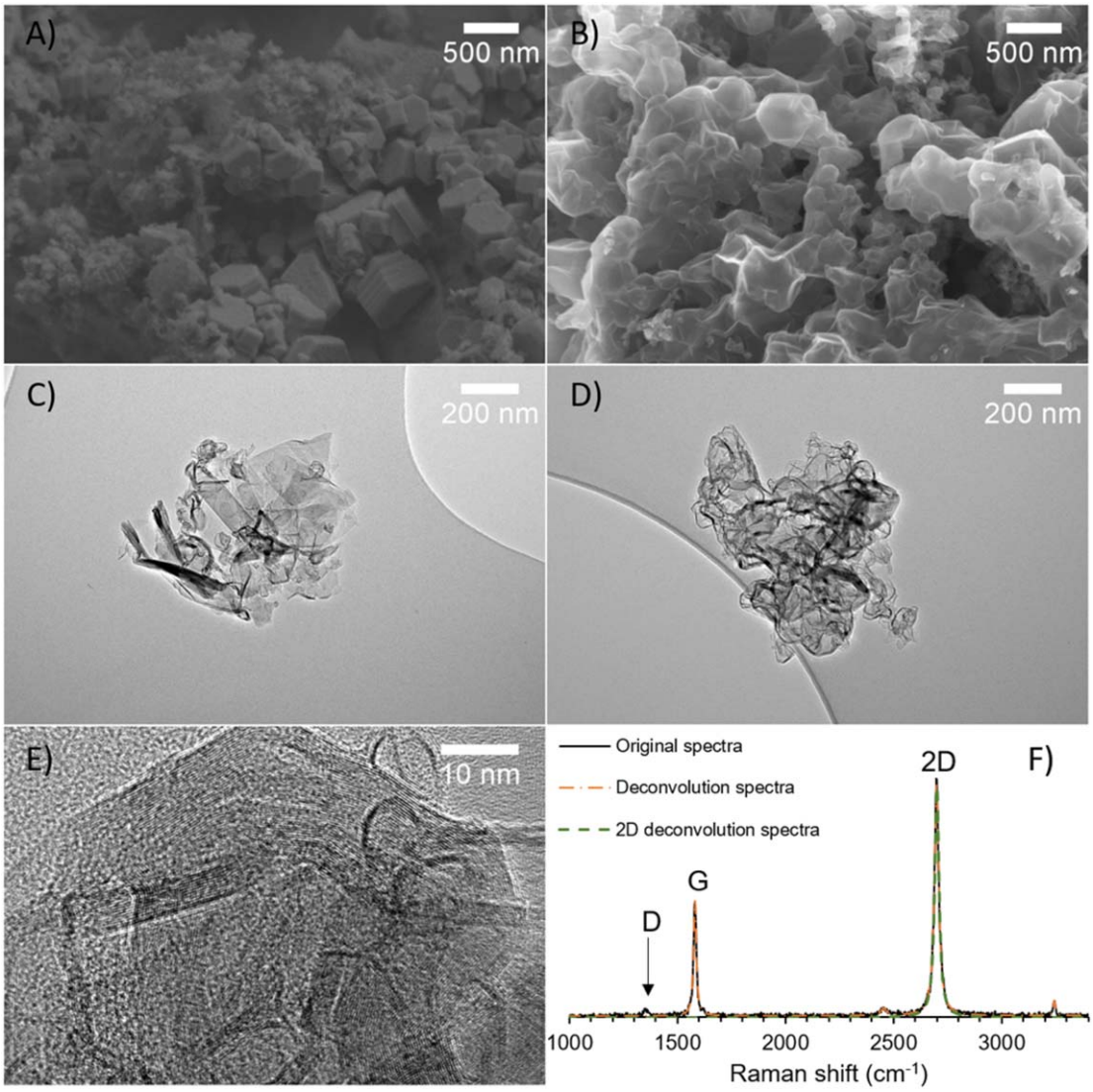

Figure 3. Scanning electron microscope (SEM) images of (A) nSiC/C composite used as precursor and (B), graphene-like carbon, (C)–(E) Transmission electron microscope (TEM) images and (F) Raman spectra of graphene-like carbon domain in the sample matrix.

initiates above 2000 °C, which is in accordance with the SiC dissociation scheme presented by Lilov *et al* (1993), proceeding through the following reactions.

$$SiC(s) \leftrightarrow Si(g) + C(s) \quad (1)$$

$$2SiC(s) \leftrightarrow SiC_2(g) + Si(l, g) \quad (2)$$

However, the rate of sublimation is typically very slow at these temperatures and complete removal of Si from SiC would take very long time unless low pressures are used. Therefore, sublimation of silicon and subsequent graphitization of SiC has been typically carried out in ultrahigh vacuum conditions (UHV 10^{-8} to 10^{-9} Torr) around 1470 K [33, 34].

According to equilibrium, the maximum solid carbon conversion (26%) with the used SiC mixing ratio is achieved at 2660 °C, while further increase in temperature declines the carbon conversion and gaseous compounds, such as SiC_2 (g), Si_2C, Si (g) and C_x (g), become predominant (figure 5). The calculated maximum carbon conversion is in a very good agreement with the experimentally determined carbon conversion of commercial SiC at 2400 °C in which 25 wt% of material was graphitized (figure 2(A)). Furthermore, the local equilibrium without the presence of Ar-atmosphere indicates that the decomposition of SiC may also lead to a formation C-Si liquid alloy [35]. Induction annealing of nSiC/C at same reaction temperature resulted complete conversion to graphene-like structures. This may indicate lower onset temperature compared to temperature predicted with thermodynamic equilibrium calculations and behavior of commercial SiC. Enhanced reaction kinetics is most likely related to the pre-ceramic, nanocrystalline features of the precursor nSiC, which lower the Si and C phase separation temperature [16]. Si begins to evaporate from the powder due its higher vapor

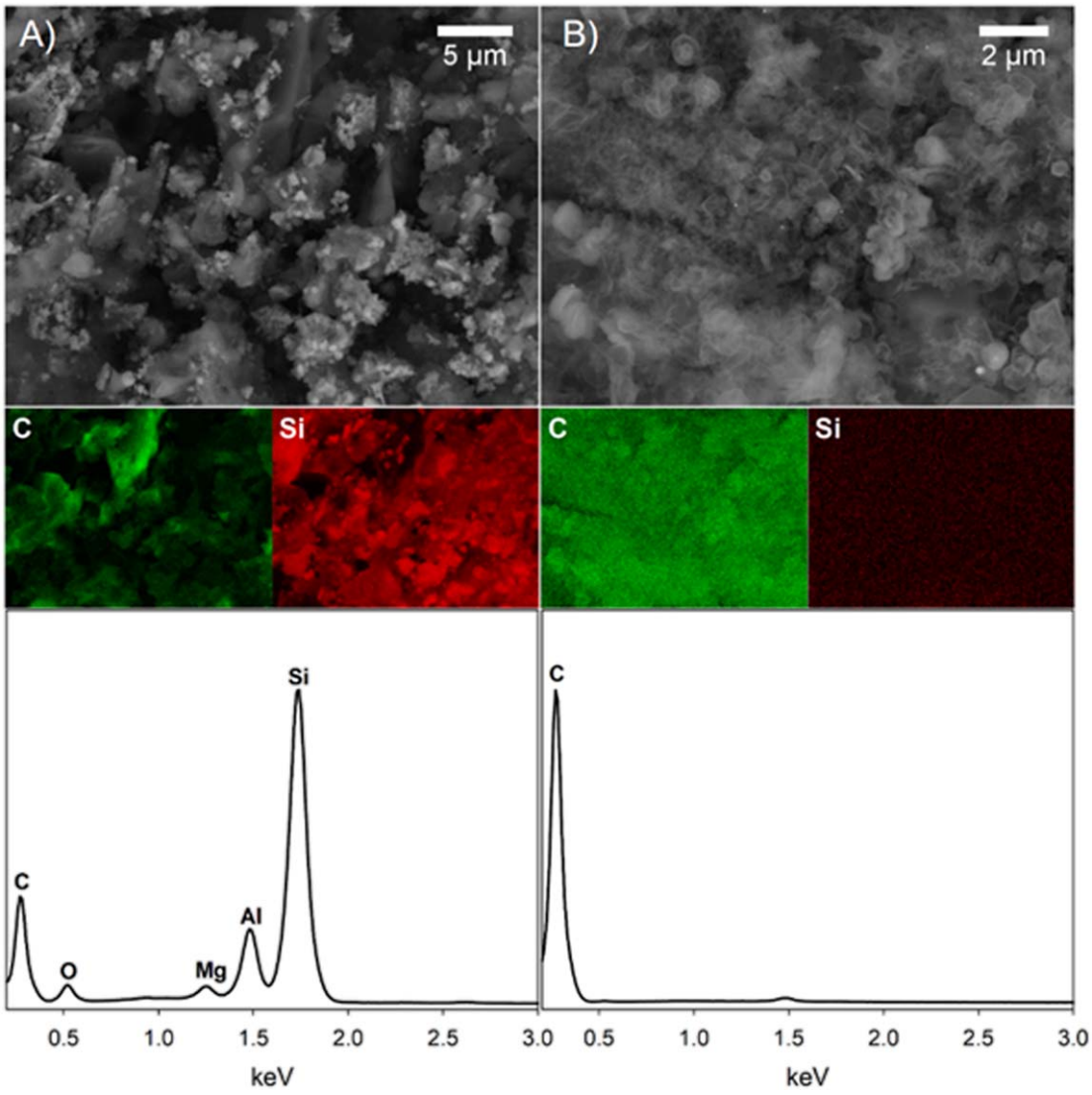

Figure 4. Energy dispersive x-ray spectroscopy analysis including backscattering images (top), elemental mappings (middle) and elemental spectrums (bottom) of the (A) nSiC/C composite and (B) graphene-like carbon.

pressure compared to the C leading to the formation of graphene and graphitic structures [2]. It has been suggested that the Si evaporates in a layer by layer fashion but the exact chemical composition of the Si atoms leaving the surface is not fully understood. In addition, the amount of free carbon seems to be an important factor affecting the growth of the graphene layers observed in the study. When the amount of free carbon was increased in pre-ceramic nSiC/C mixture produced in this study, the onset temperature for the phase separation decreased. This is most likely due to Si/C interactions, enabling the formation of the graphene-like structures already at temperatures between 1900 °C and 2600 °C [16]. The effect of free carbon is in agreement with the simulations carried out by Wang *et al* (2007) [34]. Based on the simulations the SiC surface is rapidly covered with carbon through cap nucleation of carbon once the top Si atom layer has been removed.

4. Summary

In summary, the study shows that graphene-like carbon nanostructures can be achieved from biomass-based precursors through energy efficient bottom-up synthesis procedures, magnesiothermic reduction and induction annealing. The nSiC/C composite, used as the precursor in the synthesis of graphene-like carbon nanomaterial, was obtained from sucrose and $nSiO_2$. The $nSiO_2$ was extracted from an agricultural side stream, namely barley husk. The precursor nSiC/C composed of nSiC and 21 wt% of free carbon. Crystalline and low defect graphene-like carbon, composing of nano-sized individual spherical particles 50–500 nm in size and sheet structures, was obtained through magnesiothermic reduction coupled with induction annealing. Reaction mechanism leading to the formation of graphene-like carbon was initiated by the evaporation of Si. We observed

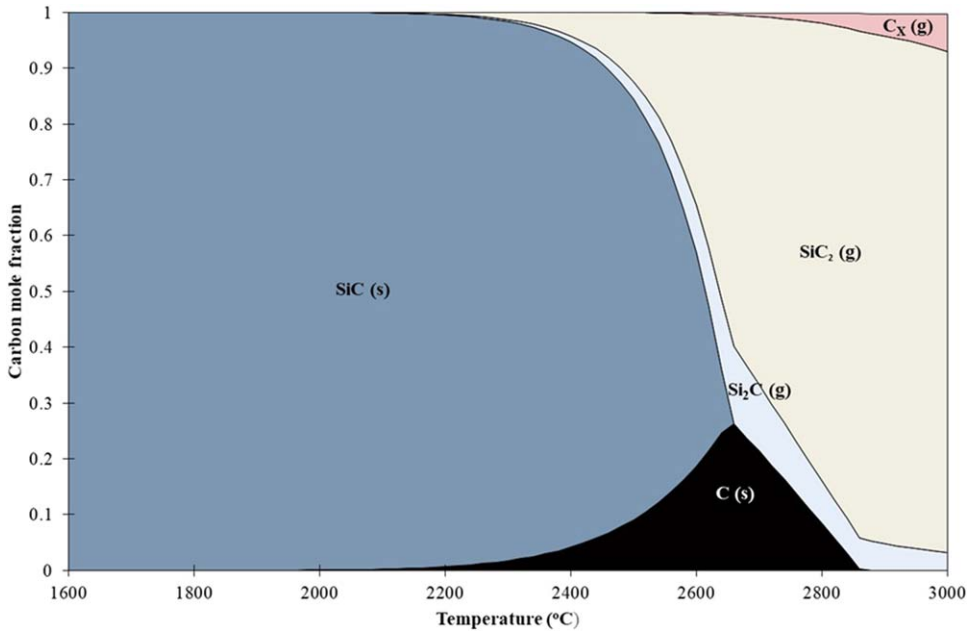

Figure 5. Thermodynamic equilibrium calculation of the phase separation of well crystalline SiC to silicon and carbon.

significant improvement in the reaction kinetics of nSiC/C compared to commercial SiC. Lowering of the phase separation temperature is related to the nanocrystalline structure of biogenic SiC and the large amount of free carbon in the nSiC/C precursor composite.

Acknowledgments

This work was supported by the Academy of Finland (grant numbers 308062 and 325495) and Business Finland (NanOhra-project). Altia Oyj is acknowledged for providing the barley husk.

ORCID iDs

Anna Lähde https://orcid.org/0000-0001-9674-4482
Sara-Maaria Alatalo https://orcid.org/0000-0001-6101-1529
Arūnas Meščeriakovas https://orcid.org/0000-0002-3257-5293

References

[1] Geim A K and Novoselov K S 2007 The rise of graphene *Nat. Mater.* **6** 183
[2] Emtsev K V *et al* 2009 Towards wafer-size graphene layers by atmospheric pressure graphitization of silicon carbide *Nat. Mater.* **8** 203
[3] Novoselov K S, Fal'ko V I, Colombo L, Gellert P R, Schwab M G and Kim K 2012 A roadmap for graphene *Nature* **490** 192
[4] Yazdi G R, Vasiliauskas R, Iakimov T, Zakharov A, Syväjärvi M and Yakimova R 2013 Growth of large area monolayer graphene on 3C-SiC and a comparison with other SiC polytypes *Carbon N. Y.* **57** 477–84
[5] Ferrari A C *et al* 2015 Science and technology roadmap for graphene, related two-dimensional crystals, and hybrid systems *Nanoscale.* **7** 4598–810
[6] Lin L, Peng H and Liu Z 2019 Synthesis challenges for graphene industry *Nat. Mater.* **18** 520–4
[7] Abdul G, Zhu X and Chen B 2017 Structural characteristics of biochar-graphene nanosheet composites and their adsorption performance for phthalic acid esters *Chem. Eng. J.* **319** 9–20
[8] Shams S S, Zhang L S, Hu R, Zhang R and Zhu J 2015 Synthesis of graphene from biomass: a green chemistry approach *Mater. Lett.* **161** 476–9
[9] Liu B, Liu Y, Chen H, Yang M and Li H 2017 Oxygen and nitrogen co-doped porous carbon nanosheets derived from Perilla frutescens for high volumetric performance supercapacitors *J. Power Sources* **341** 309–17
[10] Wang Z, Shen D, Wu C and Gu S 2018 State-of-the-art on the production and application of carbon nanomaterials from biomass *Green Chem.* **20** 5031–57
[11] Sevilla M, Sanchís C, Valdés-Solís T, Morallón E and Fuertes A B 2007 Synthesis of graphitic carbon nanostructures from sawdust and their application as electrocatalyst supports *J. Phys. Chem.* C **111** 9749–56
[12] Sun L, Tian C, Li M, Meng X, Wang L, Wang R, Yin J and Fu H 2013 From coconut shell to porous graphene-like nanosheets for high-power supercapacitors *J. Mater. Chem.* A **1** 6462–70
[13] Sevilla M and Fuertes A B 2010 Graphitic carbon nanostructures from cellulose *Chem. Phys. Lett.* **490** 63–8

[14] de Heer W A, Berger C, Ruan M, Sprinkle M, Li X, Hu Y, Zhang B, Hankinson J and Conrad E 2011 Large area and structured epitaxial graphene produced by confinement controlled sublimation of silicon carbide *Proc. Natl Acad. Sci.* **108** 16900–5 LP
[15] Speck F, Ostler M, Besendörfer S, Krone J, Wanke M and Seyller T 2017 Growth and intercalation of graphene on silicon carbide studied by low-energy electron microscopy *Ann. Phys.* **529** 1700046
[16] Miettinen M, Hokkinen J, Karhunen T, Torvela T, Pfüller C, Ramsteiner M, Tapper U, Auvinen A, Jokiniemi J and Lähde A 2013 Synthesis of novel carbon nanostructures by annealing of silicon-carbon nanoparticles at atmospheric pressure *J. Nanoparticle Res.* **16** 2168
[17] Su J, Gao B, Chen Z, Fu J, An W, Peng X, Zhang X, Wang L, Huo K and Chu P K 2016 Large-scale synthesis and mechanism of β-SiC nanoparticles from rice husks by low-temperature magnesiothermic reduction *ACS Sustain. Chem. Eng.* **4** 6600–7
[18] Omidi Z, Ghasemi A and Bakhshi S R 2015 Synthesis and characterization of SiC ultrafine particles by means of sol-gel and carbothermal reduction methods *Ceram. Int.* **41** 5779–84
[19] Yermekova Z, Mansurov Z and Mukasyan A 2010 Influence of precursor morphology on the microstructure of silicon carbide nanopowder produced by combustion syntheses *Ceram. Int.* **36** 2297–305
[20] Zhao B, Zhang H, Tao H, Tan Z, Jiao Z and Wu M 2011 Low temperature synthesis of mesoporous silicon carbide via magnesiothermic reduction *Mater. Lett.* **65** 1552–5
[21] Gerhard R 2011 *Properties and Applications of Silicon Carbide* (London UK: Intech Open) (https://doi.org/10.5772/615)
[22] Martin H-P, Ecke R and Müller E 1998 Synthesis of nanocrystalline silicon carbide powder by carbothermal reduction *J. Eur. Ceram. Soc.* **18** 1737–42
[23] Rudolf R, Mitschang P and Neitzel M 2000 Induction heating of continuous carbon-fibre-reinforced thermoplastics *Compos. Part A Appl. Sci. Manuf.* **31** 1191–202
[24] Fraysse F, Pokrovsky O S, Schott J and Meunier J-D 2009 Surface chemistry and reactivity of plant phytoliths in aqueous solutions *Chem. Geol.* **258** 197–206
[25] Umeda J and Kondoh K 2010 High-purification of amorphous silica originated from rice husks by combination of polysaccharide hydrolysis and metallic impurities removal *Ind. Crops Prod.* **32** 539–44
[26] Ortiz A L, Cumbrera F L, Sánchez-Bajo F, Guiberteau F, Xu H and Padture N P 2000 Quantitative phase-composition analysis of liquid-phase-sintered silicon carbide using the rietveld method *J. Am. Ceram. Soc.* **83** 2282–6
[27] Ortiz A, Sánchez-Bajo F, Cumbrera F and Guiberteau F 2001 X-ray powder diffraction analysis of a silicon carbide-based ceramic *Mater. Lett.* **49** 137–45
[28] Kang F and Iwashita N 2016 X-ray powder diffraction *Mater. Sci. Eng. Carbon.* 7–25 Chapter 2
[29] Gallis S, Nikas V, Eisenbraun E, Huang M and Kaloyeros A E 2009 On the effects of thermal treatment on the composition, structure, morphology, and optical properties of hydrogenated amorphous silicon-oxycarbide *J. Mater. Res.* **24** 2561–73
[30] Ingaki M and Kang F 2016 Introduction *Mater. Sci. Eng. Carbon.* Chapter 1 ISBN 978-0-12-800858-4 1–6
[31] Ferrari A C 2007 Raman spectroscopy of graphene and graphite: disorder, electron–phonon coupling, doping and nonadiabatic effects *Solid State Commun.* **143** 47–57
[32] Miettinen M, Johansson M, Suvanto S, Riikonen J, Tapper U, Pakkanen T T, Lehto V-P, Jokiniemi J and Lähde A 2011 Atmospheric pressure chemical vapour synthesis of silicon–carbon nanoceramics from hexamethyldisilane in high temperature aerosol reactor *J. Nanoparticle Res.* **13** 4631–45
[33] Sutter P 2009 How silicon leaves the scene *Nat. Mater.* **8** 171–2
[34] Wang Z, Irle S, Zheng G, Kusunoki M and Morokuma K 2007 Carbon nanotubes grow on the C Face of SiC (000$\bar{1}$) during sublimation decomposition: quantum chemical molecular dynamics simulations *J. Phys. Chem.* C **111** 12960–72
[35] Ansara M, Dinsdale I and Rand A T 1998 Definition of thermochemical and thermophysical properties to provide a database for the development of new light alloys *COST* **2**